Immobilization of rough morphotype Mycolicibacterium neoaurum R for androstadienedione production

Anqi Zhao
Zhengzhou University
Yamei Li
Zhengzhou University
Lixia Wu
Zhengzhou University
Zhi Wang
Zhengzhou University
Yongkun Lv
Zhengzhou University
Wenlong Xiong
Zhengzhou University
Mohammed Asraful Alam
Zhengzhou University
Guohua Liu
Chinese Academy of Agricultural Sciences Feed Research Institute
Jingliang Xu (xujl@zzu.edu.cn)
Zhengzhou University https://orcid.org/0000-0003-0029-5710

Research Article

Keywords: Androst-1,4-diene-3,17-dione, Cell immobilization, Perlite, Rough colony morphotype variant, Mycolicibacterium neoaurum

Posted Date: June 26th, 2023

DOI: https://doi.org/10.21203/rs.3.rs-2990936/v1

Version of Record: A version of this preprint was published at Biotechnology Letters on December 8th, 2023. See the published version at https://doi.org/10.1007/s10529-023-03448-x.

Abstract

Objectives

Enhance androstadienedione (Androst-1,4-diene-3,17-dione, ADD) production of rough-type morphotype *Mycolicibacterium neoaurum* variant by repeated-batch fermentation of immobilized cells.

Results

M. neoaurum R was a rough colony morphotype variant, obtained from routine plating of smooth *M. neoaurum* strain CICC 21097. *M. neoaurum* R showed rougher cell surface and aggregated in broth. The ADD production of *M. neoaurum* R was notably lower than that of *M. neoaurum* CICC 21097 during the free cell fermentation, but the yield gap could be erased after proper cell immobilization. Subsequently, repeated-batch fermentation by immobilized *M. neoaurum* R was performed to shorten the production cycle and enhance the bio-production efficiency of ADD. Through the optimization of the immobilization carriers and the solvents for phytosterols, the ADD productivity of *M. neoaurum* R immobilized by semi-expanded perlite reached 0.075 g/L/h during the repeated-batch fermentation for 40 days.

Conclusions

Although smooth strains that could homogenously suspended in broth seemed to be preferred in the steroid bioconversion, the rough-type strain *M. neoaurum* R might be able to find their place by proper cell immobilization.

Introduction

Steroid-based drugs have been developed as the second largest medical category after antibiotics. About 300 steroid-based drugs have been approved, with an annual output exceeding one million tons (Fernández-Cabezón et al. 2018). As the bulk platform chemicals for fine pharmaceutical steroids, steroid-based drug intermediates are indispensable in steroid industry. Although the classic steroid chemistry route that employs 16-dehydropregnenolone acetate (16-DPA) as the intermediate is dominant at present, the biosynthesis of steroid-based drug intermediates has got much attention from both laboratory researchers and pharmaceutical companies (Laveaga 2005). The bio-route shows advantages on abundant and low-cost start materials, multiple steroid drug intermediate products, ecofriendly processes, and one pot and one operation step for consecutive biochemical reactions (Zhao et al. 2021). Among the multiple biosynthesized steroid-based drug intermediates, androstadienedione (androst-1,4-diene-3,17-dione, ADD) has a large market demand, as it has been recognized as a versatile chemical serving as the precursor for many important steroid-based drugs, including progesterone, testosterone, cortisol, estradiol, cortisone, prednisolone and prednisone (Batth et al. 2020; Feng et al. 2022).

Over the decades, many microorganisms have been isolated for the production of steroid-based drug intermediates, but only strains of *Mycolicibacterium neoaurum* (basonym: *Mycobacterium neoaurum*) have been used for mass production at industrial scale (Fernández-Cabezón et al. 2018). Phytosterols are frequently used as the start material for the steroid bioconversion. Commercially, phytosterols are often obtained as a by-product or waste of vegetable oil refining industry as a mixture of β-sitosterol, stigmasterol, campesterol and brassicasterol (Almeida et al. 2020). By truncating side-chain and modifying nucleus of the steroid components of phytosterols, ADD can be produced by some mycobacteria and mycolicibacteria. The overall process of the ADD bio-production from phytosterols in mycobacteria and mycolicibacteria has been unveiled, but some steps and mechanisms are still unknown (Liu et al. 2018). Androsta-4-ene-3,17-dione (androstenedione, AD), sharing similar molecular structure and metabolic pathway, is usually produced as the byproduct in ADD-producing strains (Amin et al. 2010; Zhang et al. 2021; Zhao et al. 2022). Additionally, the aqueous solubility of phytosterols is about 2 mg/L in aqueous media, limiting the efficiency of steroid bioconversion (Josefsen et al. 2017). In order to improve the bioaccessibility of phytosterols and enhance the steroid bioconversion of mycobacteria and mycolicibacteria, varied attempts were made, mainly including the supplements of cyclodextrins (CDs), surfactants, adsorbents and oils (Zhao et al. 2021).

Although the mycobacterial and mycolicibacterial strains that employed for the bio-production of steroid-based drug intermediates were frequently classified as the rapidly growing mycobacteria (RGM), the time course of steroid bio-conversion typically reached about ten days or more with the inclusion of seed cultivation (Mancilla et al. 2018; Zhao et al. 2022). In order to accelerate the bio-process by reducing the non-productive phase and improving the operation efficiency, repeated-batch fermentation by immobilized cells has been performed in previous studies. Bagasse as the immobilization carrier increased the total ADD and AD productivity of the *Mycobacterium* sp. LZ2 co-expressing VHb and MceG by 56% and reduced the biotransformation period from 60 days to 37 days (Zhang et al. 2021). Moreover, the ADD and AD yields of *Mycobacterium* sp. DSM 2966 and *Mycobacterium* sp. DSM 2967 were enhanced by 3-4-fold after the passive adsorption onto *Luffa cylindrical* (Saab et al. 2010). The immobilization of *Mycobacterium* sp. NRRL B-3805 onto chrysotile led to higher bioconversion rates and allowed the implementation of a continuous operation mode (Wendhausen et al. 2005). Besides, multiple inorganic and organic materials, including celite, concrete, silicone rubbers, poly vinyl alcohol (PVA)/poly vinyl pyrrolidone (PVP) copolymer and hydrogels, have been served as the carriers for the immobilization of mycobacteria and mycolicibacteria during steroid bioconversion (Ahmed 2014; Amin et al. 2010; Claudino et al. 2008; Llanes et al. 2001).

Some nontuberculous mycobacteria (NTM), including *M. neoaurum*, have long been recognized as having both rough and smooth colony morphotype variants (Behra et al. 2019; Fregnan and Smith 1962). The smooth variants are homogenously suspended in flask-shaking, whereas the rough variants aggregate (Clary et al. 2018). Might due to that, the smooth variants seemed to be preferred in the steroid bioconversion. *Mycobacterium* sp. VKM Ac-1815D formed both rough and smooth colonies on agar after the chemical agents and UV irradiation mutagenization, but only smooth colonies were picked up and tested for sterol-transforming activities (Donova et al. 2005). In this study, a rough colony morphotype

variant, termed as *M. neoaurum* R, was isolated in the routine plating of the smooth *M. neoaurum* CICC 21097. *M. neoaurum* R and *M. neoaurum* CICC 21097 accumulated ADD as the major product in the phytosterols bioconversion. The ADD production of *M. neoaurum* R was inferior to *M. neoaurum* CICC 21097 during the free cell fermentation, but after proper cell immobilization, the rough *M. neoaurum* R showed more stable and considerable ADD production than *M. neoaurum* CICC 21097, suggesting the potential of the rough variants immobilization in the steroid bio-conversion. To further enhance the ADD productivity of *M. neoaurum* R in repeated-batch fermentation, the immobilization carriers and the co-solvents of phytosterols were optimized.

Materials and methods

Chemicals and materials

Phytosterols (mainly sterol components including β-sitosterol 33.6%, stigmasterol 30.9%, campesterol 3.5% and brassicasterol 3.2%) were purchased from HSF Biotech (Shanxi, China). Soybean meal was from Hongrun Baoshun Technology (Beijing, China). HP-β-CD (molar weight 1447, with 0.67 molar substitution of the hydroxypropyl moiety) was purchased from Zhiyuan Biotechnology (Shandong, China). HPD826 (purity ≥ 98%) was purchased from Miaoyang Chemical (Hebei, China). Sodium stearyl lactate were purchased from Shanjiaren Food (Henan, China). Semi-expanded perlite (particle size 5–10 mm) and lava rock (particle size 5–10 mm) were purchased from Mingyang Garden (Taobao, China). Expandable polyethylene and luffa sponge were collected from local market and cut into small pieces (particle size ~ 10 mm). Other chromatographic pure reagents and analytical grade reagents were purchased from Macklin (Shanghai, China). PCR Enzymes and Bacteria DNA kit were from Sangon Biotech (Shanghai, China)

Stains, media and growth conditions

M. neoaurum CICC 21097 was purchase from China Center of Industrial Culture Collection (CICC), showing smooth colony morphotypes. *M. neoaurum* R was a spontaneous mutant of *M. neoaurum* CICC 21097, showing rough colony morphotypes. *M. neoaurum* R was deposited in China Center for Type Culture Collection with the strain number CCTCC M 2021383.

The chromosomal DNAs of *M. neoaurum* CICC 21097 and *M. neoaurum* R were extracted and used as templates to amplify 16S rDNA sequences with the bacterial 16S rDNA universal primers 27F (AGAGTTTGATCMTGGCTCAG) and 1429R (GGTTACCTTGTTACGACTT) (Duong et al. 2021). The PCR products were sequenced by Sangon Biotech. The sequence data of 16S rDNAs from *M. neoaurum* CICC 21097 and *M. neoaurum* R were submitted to GenBank, and their accession numbers were OQ346110 and OQ346103, respectively.

M. neoaurum CICC 21097 and *M. neoaurum* R were maintained and rejuvenated in LB medium (10 g/L peptone, 5 g/L yeast extract and 10 g/L NaCl). For steroid bioconversion, a loop of *M. neoaurum* cell colonies were inoculated into tube containing 3 mL LB medium for 48 h at 30℃ and 200 rpm, followed

by the dilution into 30 mL seed medium (25.0 g/L fructose, 10.0 g/L peptone, 6.0 g/L yeast extract and 10.0 g/L NaCl) for 36 h. Then, 3 mL seed culture was inoculated into 30 mL fermentation medium (25.0 g/L fructose, 14.4 g/L $(NH_4)_2HPO_4$, 9.6 g/L soybean meal, 10.0 g/L NaCl, 3 g/L K_2HPO_4, 0.2 g/L $MgSO_4$, 5×10^{-4} g/L $MnCl_2{\cdot}4H_2O$ and 5 g/L phytosterols, pH 7.5) in a 250 mL flask for 96 h at 30℃ and 200 rpm.

Cell immobilization and repeated-batch fermentations

Immobilization carriers, including semi-expanded perlite, lava rock, activated carbon, expandable polyethylene and luffa sponge, were washed three times, dried at 60℃ and sterilized at 121 ℃ for 20 min before used. The carrier PVA hydrogel was prepared by adding 2.5 g PVA into 22.5 g ddH_2O, stiring at 140 ℃ to clear and transparent solution, removing bubbles by ultrasound, and then pouring into mold and placing at -20 ℃ for 12 h; the PVA hydrogel was cut into small squares with a length and width of 10 mm for use (Zhang et al. 2019). For *M. neoaurum* CICC 21097 and *M. neoaurum* R immobilization, carriers were supplemented into fermentation media. The supplements of semi-expanded perlite, lava rock and activated carbon were 160 g/L (Lyew et al. 2007), expandable polyethylene and luffa sponge were 5 g/L (Zhang et al. 2021), and PVA hydrogel were 200 g/L. After a batch fermentation for 96 h, the broth was removed and the carriers were washed by sterilized ddH_2O for three times; then 30 mL fresh fermentation medium was replenished for the repeated-batch fermentation. Samples was taken to detect the yield of ADD and androsta-4-ene-3,17-dione (AD) after each batch of fermentation, and all results were an average of triplicate experiments.

Optimization for the ADD production by immobilized M. neoaurum R

The supplement of semi-expanded perlite and co-solvents for phytosterols were optimized to enhance the ADD production by immobilized *M. neoaurum* R by one-factor-at-a-time (OFAT) experiment and orthogonal array testing. Different amount of semi-expanded perlite (0, 80, 160, 250, 340 and 420 g/L) were supplemented into fermentation media to determine the influence of the immobilization carrier on ADD production. Sodium stearoyl lactylate (SSL), macroporous resin HPD826 and hydroxylpropyl-β-cyclodextrin (HP-β-CD) were employed as co-solvents for phytosterols. Co-solvents were supplied to the fermentation media that contained 160 g/L semi-expanded perlite in different co-solvent/phytosterols ratios (1:2, 1:1, 2:1 and 4:1, w/w). The effects of phytosterols concentrations (5, 10, 15, 20 g/L) were investigated as well, in fermentation media containing equal amounts of HP-β-CD as phytosterols and 160 g/L semi-expanded perlite. According to the result of the OFAT experiments, an orthogonal $L_9(3^3)$ assay was designed on the semi-expanded perlite amount (A), phytosterols concentration (B) and HP-β-CD/phytosterols ratio (C) (Table 1). The range method was used for the results of orthogonal array testing (Fang et al. 2018).

Table 1
Orthogonal design and experimental results

Test No.	A semi-expanded perlite amount (g/L)	B phytosterols concentration (g/L)	C HP-β-CD/phytosterols ratio (w/w)	ADD (g/L)
1	80	10	1:1	2.14 ± 0.04
2	80	15	2:1	4.39 ± 0.02
3	80	20	4:1	6.17 ± 0.18
4	160	10	2:1	3.20 ± 0.06
5	160	15	4:1	4.18 ± 0.28
6	160	20	1:1	3.21 ± 0.02
7	250	10	4:1	3.61 ± 0.28
8	250	15	1:1	3.17 ± 0.11
9	250	20	2:1	4.36 ± 0.04
k1	4.23 ± 0.08	2.98 ± 0.10	2.84 ± 0.06	
k2	3.53 ± 0.11	3.91 ± 0.05	3.98 ± 0.03	
k3	3.71 ± 0.07	4.58 ± 0.05	4.65 ± 0.12	
R	0.7	1.6	1.81	

Analytical methods

ADD and AD were analyzed by HPLC (Agilent 1260, USA). Broth was extracted with twice the volume of ethyl acetate, and the upper phase were separated and filtrated for HPLC analysis. The HPLC separation and quantitation was realized on an Agilent Eclipse Plus C18 column (5 μm, 250 mm × 4.6 mm, USA) at 30 °C and 70% methanol aqueous solution was used as mobile phase at a flow rate of 1 mL/min. ADD and AD were detected at 254 nm, and the spectra were recorded online (Shao et al. 2015). The molar product yield of ADD was calculated using the following formula: ADD molar yield% = $C_{ADD}/M_{ADD}/(C_{PS}/M_{PS}) \times 100\%$, where C_{ADD} and C_{PS} were the concentration (g/L) of ADD and the total

sterol components of phytosterols, respectively; and M_{ADD} and M_{PS} are the molar masses (g/mol) of ADD and the total sterol components of phytosterols, respectively (Zhang et al. 2021).

Scanning electron microscopy (SEM) were employed to visualize the microstructures of *M. neoaurum* CICC 21097, *M. neoaurum* R and *M. neoaurum* R that was immobilized onto semi-expanded perlite. Cells of *M. neoaurum* CICC 21097 and *M. neoaurum* R were collected after the cultivation in LB broth for 48 h at 30°C and 200 rpm, and the *M. neoaurum* R immobilized by semi-expanded perlite were collected after ten-repeated-batch fermentation. The specimens were prepared as described previously (Wang et al. 2018). Briefly, samples were washed by PBS, fixed with 2.5% (v/v) glutaraldehyd and 1% (v/v) OsO4, dehydrated with gradually increasing concentrations of ethanol aqueous solution and isoamyl acetate. Then, samples were dried by critical point method, coated with gold-palladium and imaged by SEM (Hitachi SU8010, Japan) operated under high vacuum with an acceleration voltage of 5.0 kV. The carried semi-expanded perlite was imaged by SEM as well, after it was washed by ddH_2O, dried and coated with gold-palladium.

Results

Isolation of rough variant M. neoaurum R

M. neoaurum R, which was characterized by the rough and dry texture on agar plates, was obtained from a single rough colony during the routine plating of the smooth *M. neoaurum* CICC 21097 (Fig. 1). The rough cell morphotype of *M. neoaurum* R were stable over the multiple passages (Supplementary Fig. 1). The 16S rDNA sequencing and alignment confirmed that *M. neoaurum* R (OQ346103) and *M. neoaurum* CICC 21097 (OQ346110) were highly homologous, although the two isolates illustrated different phenotypes. In flask-shaking, *M. neoaurum* R tended to aggregate (Fig. 1a). In sharp contrast, *M. neoaurum* CICC 21097 which formed small smooth and moisture colonies on agar plates and homogenously suspended in broth (Fig. 1b). In SEM images, *M. neoaurum* R and *M. neoaurum* CICC 21097 both showed rods-shaped, but the cell surface of *M. neoaurum* R seemed rougher, implying that *M. neoaurum* R and *M. neoaurum* CICC 21097 might have different cell surface properties (Fig. 1).

ADD was accumulated by both *M. neoaurum* R and *M. neoaurum* CICC 21097 as the major product in fermentation medium. Small amount of androsta-4-ene-3,17-dione (AD), another C-19 steroid drug intermediate sharing similar molecular structures and metabolic pathways with ADD, was produced as the by-product. As shown in Fig. 2a, 0.02–0.06 g/L ADD and AD were produced by the two strains at 24 h. Then the AD yield stopped increasing, whereas ADD was promptly accumulated. At 96 h, the ADD yield of *M. neoaurum* R was 0.43 g/L, which was notably lower than that of *M. neoaurum* CICC 21097 (0.62 g/L). The increase of ADD production of *M. neoaurum* R and *M. neoaurum* CICC 21097 almost stalled after 96 h, suggesting that the fermentation could be terminated at 96 h. The notable lower ADD yield of *M. neoaurum* R might related to the formation of cell clumps in media (Fig. 1a); the clumps of rough *M. neoaurum* R probably further hindered the uptake of the highly hydrophobic phytosterols which tended to clump and disperse poorly in aqueous (Malaviya and Gomes 2008).

Semi-expanded perlite as carrier for M. neoaurum R immobilization

Repeated-batch fermentation, in which immobilized cells are used as inocula for subsequent batches, is an effective way to shorten the production cycle and enhance the bio-production efficiency (Zhou et al. 2020). Hence, several inorganic and organic materials, including semi-expanded perlite, lava rock, activated carbon, expandable polyethylene, PVA hydrogel and luffa sponge, were employed as the carriers for the immobilization of *M. neoaurum* R and *M. neoaurum* CICC 21097 (Fig. 3).

In the present of semi-expanded perlite and lava rock as the immobilization carriers, the ADD yields of *M. neoaurum* CICC 21097 were slightly enhanced in the first batch, respectively reaching 0.70 and 0.74 g/L, comparing with the free cell fermentation. However, the ADD yields of *M. neoaurum* CICC 21097 were obviously hindered by the carriers activated carbon, expandable polyethylene, PVA hydrogel and luffa sponge (Fig. 3). Although *M. neoaurum* CICC 21097 immobilized by lava rock had an excellent performance in the first batch, the ADD yields precipitously dropped and the AD yields slightly increased in the following two batches. When semi-expanded perlite as the carrier, the ADD yields of immobilized *M. neoaurum* CICC 21097 was moderately decreased to 0.46 g/L in Batch 3. The batch yield of byproduct AD yield of *M. neoaurum* CICC 21097 immobilized by semi-expanded perlite was about 0.05 g/L. Since *M. neoaurum* CICC 21097 immobilized by semi-expanded perlite illustrated the highest average batch production of ADD and lowest byproduct proportion in two steroid products, semi-expanded perlite was chosen as the best carrier for *M. neoaurum* CICC 21097 immobilization.

Significantly, in the present of the same investigated carrier, the ADD productions of *M. neoaurum* R and *M. neoaurum* CICC 21097 were quite similar, in contrast to the notable gap of ADD yields of the two strains in free cell fermentation (Fig. 3). Especially, the ADD production of *M. neoaurum* R reached 0.69 g/L in the present of semi-expanded perlite in the first batch (Fig. 2b), which was the highest among the ADD productions of the immobilized *M. neoaurum* R. The cycling performances of *M. neoaurum* R immobilized by semi-expanded perlite, lava rock, activated carbon, expandable polyethylene or luffa sponge were notably better than those of *M. neoaurum* CICC 21097 that was immobilized by the same carrier. The ADD yields of *M. neoaurum* R immobilized by expandable polyethylene and luffa sponge were almost constant and even increased during the three repeated batches, respectively. Although the ADD production of perlite-immobilized *M. neoaurum* R slightly decreased to 0.59 g/L in Batch 3, the average batch yield of ADD was the highest among the immobilized *M. neoaurum* R and *M. neoaurum* CICC 21097. Additionally, the average batch yield of byproduct AD of the *M. neoaurum* R immobilized by semi-expanded perlite, lava rock, activated carbon, expandable polyethylene or luffa sponge were lower than those of *M. neoaurum* CICC 21097 immobilized by the same carrier. Among them, the average AD yield of perlite-immobilized *M. neoaurum* R was the lowest, reaching 0.026 g/L (Fig. 3). Therefore, semi-expanded perlite and *M. neoaurum* R were chosen as the best combination for repeated-batch fermentation to produce ADD in this study.

Optimization of ADD accumulation by immobilized M. neoaurum R

In order to improve the ADD accumulation of immobilized *M. neoaurum* R, the additions of semi-expanded perlite for cell immobilization and co-solvents for phytosterols were optimized by the one-factor-at-a-time (OFAT) experiment and orthogonal array testing (Fig. 4 and Table 1). The investigated co-solvents included sodium stearoyl lactylate (SSL), macroporous resin HPD826 and hydroxylpropyl-β-cyclodextrin (HP-β-CD).

As shown in Fig. 4, with the increased of semi-expanded perlite amount, the ADD yield of *M. neoaurum* R increased, but no obviously increase could be observed when the addition of the carrier was more than 160 g/L. SSL is a surfactant, which could help steroids dispense in aqueous media by forming oil-in-water (O/W) emulsion (Monu et al. 2008). When SSL/phytosterols ratios (w/w) were 2:1 and 1:1, the ADD yields were about 0.70 g/L, which was similar to the yield in media without SSL. However, with the further increase of SSL, the yields decreased; and no ADD was generated when the ratio of SSL/phytosterols reached 4:1. Hence, SSL as co-solvent could not enhance the ADD biosynthesis of the perlite-immobilized *M. neoaurum* R. Resins were employed as adsorbents for steroids in several researches on steroid biotransformation (Molchanova et al. 2007; Wang et al. 2021). In fermentation medium containing the equal amount of macroporous resin HPD826 as phytosterols, ADD reached 1.11 g/L, which was 60.9% higher than that in media without HPD826. When the HPD826/phytosterols ratio (w/w) further increased to 4:1, the ADD production was further increased to 1.41 g/L. The yields of byproduct AD were increased with the supplement of HPD826 as well, reaching 0.26 g/L when HPD826/phytosterols ratio (w/w) was 4:1. However, the structure of semi-expanded perlite broke down after about three weeks of repeated-batch fermentation, might due to the strong adsorption of HPD826. Therefore, HPD826 was not the desired co-solvent of phytosterols for the bioconversion by perlite-immobilized *M. neoaurum* R. HP-β-CD contains a hydrophilic outside and a hydrophobic central cavity, which could form inclusion complexe with phytosterols (Su et al. 2020). HP-β-CD could dramatically increase the ADD yield of the perlite-immobilized *M. neoaurum* R without any side-effect on the immobilization carrier. In fermentation medium containing 5 g/L HP-β-CD and 10 g/L phytosterols, ADD yield reached 1.58 g/L, which was roughly double the data obtained in media without HP-β-CD. With the HP-β-CD/phytosterols ratio (w/w) increased to 4:1, the ADD yield reached 3.62 g/L, with a molar yield of 73.7%. Additionally, as the phytosterols content increased from 5 to 20 g/L in fermentation media containing equal amounts of HP-β-CD as phytosterols, the ADD yields increase from 1.20 g/L to 2.88 g/L, but the ADD molar yield decreased from 48.9–29.3%.

The semi-expanded perlite amount, phytosterols concentration and HP-β-CD/phytosterols ratio showed positive effects on the ADD production of the perlite-immobilized *M. neoaurum* R, thus those factors were selected for the $L_9(3^3)$ orthogonal design (Table 1). The levels of the factors were mainly selected by ADD production, and took ADD molar yield, byproduct yield and cost were into consideration. In result of the $L_9(3^3)$ orthogonal test, the ADD production of Test 3 reached 6.17 g/L, which was the highest among the tests. The ADD molar yield of Test 3 was 62.8%, which was slightly lower than the highest data 73.5% of Test 8. The byproduct AD of Test 3 was 0.72 g/L, which only occupied 10.45% in total C19-steroid product (AD and ADD). The ranges (R) reflected the factors' sensitivity to the experimental result

according to the orthogonal experiment (Pan et al. 2022), thus impacts of three factors on ADD productions could be ranked as: HP-β-CD/phytosterols ratio > phytosterols concentration > semi-expanded perlite amount. According to the analysis of *k* values, the optimal levels of the factors HP-β-CD/phytosterols ratio (w/w), phytosterols concentration and semi-expanded perlite amount respectively were 4, 20 g/L and 80 g/L, which are coincident with the levels of Test 3 in Table 1.

Extended repeated-batch fermentation of immobilized M. neoaurum R

Extended repeated-batch process (10 batches, 40 days) of *M. neoaurum* R immobilized by semi-expanded perlite was carried out in fermentation media containing 20 g/L phytosterols, 80 g/L HP-β-CD and 80 g/L semi-expanded perlite (Fig. 5a). The batch production of ADD was peaked at Batch 2, reaching 7.90 g/L, with a ADD molar yield of 80.5%, which was 28.0% higher than that of Batch 1. Then slightly fluctuations of ADD yields were observed during the repeated batch process, but the average ADD batch yield reached 7.22 g/L. The byproduct AD was produced with an average batch yield of 0.75 g/L, which was almost one-tenth of the average ADD yield. Surprisingly, the ADD yield of Batch 10 was maintained 6.55 g/L, which was higher than that of Batch 1. The guaranteed ADD yields of the ten batches fermentation indicated the possibility of more prolonged processes.

Semi-expanded perlite was changed from white to yellow color after the repeated-batch fermentation (Fig. 5a and 5c). The SEM image of the carrier suggested that the porous structure of semi-expanded perlite provided suitable beds for surface binding and the entrapment of *M. neoaurum* R. The adequate retention of cells scattered on the carriers after the ten-batch fermentation, which supported strong ADD production capacity in the ten repeat-batch fermentation (Fig. 5c).

Discussion

Perlite is a glassy volcanic rock with a rhyolitic composition. Commercially perlite includes any volcanic glass that will expand when heated quickly, forming a lightweight frothy material (Ivankovic et al. 2010). Perlite usually goes to horticulture and construction industries, but several researches successfully used perlite as a carrier for cell immobilizations. For example, the stability for oil degradation by *Pseudomonas* sp. was enhanced by cell immobilized onto perlite (Emtiazi et al. 2005). A column system using perlite-immobilized *Saccharomyces cerevisiae* as stationary phase was designed for the decontamination of aflatoxin M1 in milk (Foroughi et al. 2018). Perlite was selected as the best support material for the immobilization of *Mycobacterium austroafricanum* IFP 2012 that was capable of mineralizing methyl *tert*-butyl ether (Lyew et al. 2007). According to the degree of expansion, perlite can be sub-categorized into semi-expanded perlite and expanded perlite, and the density and strength of semi-expanded perlite are superior to expanded perlite. In this study, the ADD yields of *M. neoaurum* R immobilized by expanded perlite (data not shown) and semi-expanded perlite were both desirable, but the structure of expanded perlite broke down after about three repeated batches of fermentation. Thereby, semi-expanded perlite was employed as carrier for the immobilization of *M. neoaurum* R in this research.

The extremely low aqueous solubility of phytosterols greatly limits the substrate bioaccessibility to *M. neoaurum* during the steroid biotransformation. Multiple co-solvents of phytosterols were investigated to enhance the steroid biotransformation (Zhao et al. 2021). Among the co-solvents, HP-β-CD that contains hydrophilic outside and hydrophobic central cavity was frequently used. The proteome analysis of *M. neoaurum* MNR M3C2 suggested that HP-β-CD not only could improve the solubilization of phytosterols, but also could up-regulate the expression of most proteins involved in steroid metabolism (Su et al. 2020). In this study, the ADD yield of immobilized *M. neoaurum* R was dramatically enhanced by HP-β-CD. The HP-β-CD was supplemented in a mass ratio (w/w) of 4:1 to phytosterols in this study, which was roughly equivalent to the 1:1 molar ration (mol/mol) of HP-β-CD to phytosterols. Despite that the trend of Fig. 3 and the results of some previous researches (Gao et al. 2015; Shen et al. 2012) implied that the ADD yield of *M. neoaurum* R might be further enhanced by the higher molar ration of HP-β-CD/phytosterols, but considering the cost, the upper limit of HP-β-CD/phytosterols mass ratio (w/w) was set as 4:1 in this study.

M. neoaurum R was a rough variant of the smooth ADD-producing strain *M. neoaurum* CICC 21097. The SEM image displayed that the cell surface morphotype of *M. neoaurum* R was rougher than that of *M. neoaurum* CICC 21097. Similar cell surface morphotype change was also observed in smooth-to-tough morphotype alteration of *Mycobacterium mucogenicum* (Kang et al. 2022) Researches on *M. mucogenicum*, *Mycobacterium abscessus*, *Mycolicibacterium smegmatis* and *Mycobacterium avium* strains revealed that the smooth-to-tough morphotype alterations should be related to the reduction of cell wall glycopeptidolipid (GPL) production (Das et al. 2018; Gutiérrez et al. 2018). However, surveying the *gpl* locus shows that several of the genes are absent in *M. neoaurum*, suggesting that factors other than genes in the *gpl* locus might influence the colony morphotype (Behra et al. 2019). Hence, the smooth-to-tough morphotype alterations in *M. neoaurum* CICC 21097 and *M. neoaurum* R was probably resulted from the changes in the cell surface, although it might not GPL.

ADD was the major product of *M. neoaurum* R and *M. neoaurum* CICC 21097, although small amount of AD was synthesized in fermentation media. Due to the shared metabolic pathway, ADD and AD were frequently produced together (Amin et al. 2010; Zhang et al. 2021; Zhao et al. 2022), but AD is around one tenth of the yield of ADD in this study. Intriguingly, the ADD production of *M. neoaurum* R was notably lower than that of *M. neoaurum* CICC 21097 in free cell fermentation, but the gap of yield could be erased by the addition of the immobilization carriers. The scatter of *M. neoaurum* R on carriers probably reduced the formation of the large clumps that might hinder the uptake of the hydrophobic phytosterols (Malaviya and Gomes 2008). Additionally, perhaps owing to the different cell surface properties, the cycling performance of the immobilized *M. neoaurum* R were usually better than the immobilized *M. neoaurum* CICC 21097. After optimizing the carrier of cell immobilization and the co-solvents of phytosterols, the ADD productivity of *M. neoaurum* R immobilized by semi-expanded perlite reached 0.075 g/L/h during the repeated-batch fermentation for 40 days. In past decades, several studies focused on the bio-production of steroid-based drug intermediates by immobilized bacteria. However, calculating from the data in the reports, the productivities (g/L/h) were usually of the order of 10^{-4} to 10^{-3}, which were not

desirable for mass production (Amin et al. 2010; Claudino et al. 2008; Saab et al. 2010; Wendhausen et al. 2005). Until recently, the AD and ADD total productivity was greatly enhanced to 0.069 g/L/h during the 37 days' repeated-batch fermentation of *Mycobacterium* sp. LZ2 that co-expressed VHb and MceG and was immobilized by bagasse (Zhang et al. 2021). Therefore, comparing with the previous reports, the ADD production and productivity of *M. neoaurum* R immobilized by semi-expanded perlite was outstanding. Moreover, the stable batch yields of *M. neoaurum* R immobilized by semi-expanded perlite suggested the possibility of more prolonged processes.

Conclusions

M. neoaurum R, a rough colony variant of the smooth *M. neoaurum* strain CICC 21097, showed rougher cell surface morphotype than the parent strain in SEM image. Might owing to the different cell surface characters, the immobilized *M. neoaurum* R showed higher ADD batch yields and better cycling performance than *M. neoaurum* CICC 21097 immobilized by the same carrier. The ADD productivity of *M. neoaurum* R immobilized by semi-expanded perlite reached 0.075 g/L/h during the repeated-batch fermentation for 40 days, suggesting the potential of rough *M. neoaurum* R immobilized on semi-expanded for prolonged repeated-batch fermentation processes. Moreover, although smooth strains that could homogenously suspended in broth seemed to be preferred in the steroid bioconversion, the rough-type variants of mycobacteria and mycolicibacteria might be able to find their place in the steroid bioconversion by proper cell immobilization.

Declarations

Acknowledgements Funding was provided by grants from the National Natural Science Foundation of China (31800034 and 22078308); Henan Provincial Key Research and Development Program (212102310865); the Open ProjectProgram of Key Laboratory of Feed Biotechnology, the Ministry of Agriculture and Rural Affairs of the People's Republic of China; Innovation Leadership Program in Sciences and Technologies for Central Plains Talent Plan (214200510009); Program for Science & Technology Innovative Research Team in the University of Henan Province (22IRTSTHN007); Key Program of Henan Provincial Science and Technology R&D Plan Joint Fund for Cultivation of Superior Disciplines 222301420008 .

Author contribution YML, LW and ZW performed the experiments. WX and MA contributed analytical methods. YML and YKL analyzed data. JLX, GHL and AQZ conceived and designed research. AQZ wrote the manuscript and supervised the research. All authors read and approved the manuscript.

Data availability All data generated or analyzed during this study are included in this published article (and its supplementary information file)

Ethics approval This article does not contain any studies with human participants or animals performed by any of the authors.

Competing interest The authors declare no competing financial interests.

References

1. Ahmed EM (2014) Utilization of concrete as a carrier for bacterial cells during bioconversion of some sterols. Int J Chem Sci 12:413–428
2. Almeida CAS, Baggio SR, Mariutti LRB, Bragagnolo N (2020) One-step rapid extraction of phytosterols from vegetable oils. Food Res Int 130:108891. https://doi:10.1016/j.foodres.2019.108891
3. Amin H, El-Hadi A, Mohamed S (2010) Immobilization of *Mycobacterium* sp. NRRL B-3805 cells onto radiation crosslinked PVA/PVP hydrogels for production of androstenones from β-sitosterol. Aust J Basic Appl Sci 4:2196–2205
4. Batth R, Nicolle C, Cuciurean IS, Simonsen HT (2020) Biosynthesis and industrial production of androsteroids. Plants (Basel Switzerland) 9(9):1144. https://doi:10.3390/plants9091144
5. Behra PRK, Pettersson BMF, Ramesh M, Dasgupta S, Kirsebom LA (2019) Insight into the biology of *Mycobacterium mucogenicum* and *Mycobacterium neoaurum* clade members. Sci Rep 9(1):19259. https://doi:10.1038/s41598-019-55464-5
6. Clary G, Sasindran SJ, Nesbitt N, Mason L, Cole S, Azad A, McCoy K, Schlesinger LS, Hall-Stoodley L (2018) *Mycobacterium abscessus* smooth and rough morphotypes form antimicrobial-tolerant biofilm phenotypes but are killed by acetic acid. Antimicrob Agents Chemother 62(3):e01782–e01717. https://doi:10.1128/aac.01782-17
7. Claudino MJ, Soares D, Van Keulen F, Marques MP, Cabral JM, Fernandes P (2008) Immobilization of mycobacterial cells onto silicone–assessing the feasibility of the immobilized biocatalyst in the production of androstenedione from sitosterol. Bioresour Technol 99(7):2304–2311. https://doi:10.1016/j.biortech.2007.05.007
8. Das S, Pettersson BMF, Behra PRK, Mallick A, Cheramie M, Ramesh M, Shirreff L, DuCote T, Dasgupta S, Ennis DG, Kirsebom LA (2018) Extensive genomic diversity among *Mycobacterium marinum* strains revealed by whole genome sequencing. Sci Rep 8(1):12040. https://doi:10.1038/s41598-018-30152-y
9. Donova MV, Gulevskaya SA, Dovbnya DV, Puntus IF (2005) *Mycobacterium* sp. mutant strain producing 9α-hydroxyandrostenedione from sitosterol. Appl Microbiol Biotechnol 67(5):671–678. https://doi:10.1007/s00253-004-1808-y
10. Duong B, Nguyen HX, Phan HV, Colella S, Trinh PQ, Hoang GT, Nguyen TT, Marraccini P, Lebrun M, Duponnois R (2021) Identification and characterization of Vietnamese coffee bacterial endophytes displaying in vitro antifungal and nematicidal activities. Microbiol Res 242:126613. https://doi:10.1016/j.micres.2020.126613
11. Emtiazi G, Shakarami, Nahvi, Mirdamadian I (2005) Utilization of petroleum hydrocarbons by *Pseudomonas* sp. and transformed *Escherichia coli*. Afr J Biotechnol 4(2):172–176

12. Fang S, Gu W, Chen L, Yu Z, Dai M, Lin Y, Liao Y, Ma X (2018) Ultrasonic pretreatment effects on the co-pyrolysis of municipal solid waste and paper sludge through orthogonal test. Bioresour Technol 258:5–11. https://doi:10.1016/j.biortech.2018.02.120
13. Feng J, Wu Q, Zhu D, Ma Y (2022) Biotransformation enables innovations toward green synthesis of steroidal pharmaceuticals. Chemsuschem 15(9):e202102399. https:// 10.1002/cssc.202102399
14. Fernández-Cabezón L, Galán B, García JLG (2018) New insights on steroid biotechnology. Front Microbiol 9:958
15. Foroughi M, Sarabi Jamab M, Keramat J, Foroughi M (2018) Immobilization of *Saccharomyces cerevisiae* on perlite beads for the decontamination of aflatoxin M1 in milk. J Food Sci 83(7):2008–2013. https://doi:10.1111/1750-3841.14100
16. Fregnan GB, Smith DW (1962) Description of various colony forms of mycobacteria. J Bacteriol 83(4):819–827. https:// 10.1128/jb.83.4.819-827.1962
17. Gao X, Feng J, Wang X, Hua Q, Wei D (2015) Enhanced steroid metabolites production by resting cell phytosterol bioconversion. Chem Biochem Eng Q 29(4):567–573
18. Gutiérrez AV, Viljoen A, Ghigo E, Herrmann JL, Kremer L (2018) Glycopeptidolipids, a double-edged sword of the *Mycobacterium abscessus* complex. Front Microbiol 9:1145. https://doi:10.3389/fmicb.2018.01145
19. Ivankovic T, Hrenovic J, Sekovanic L (2010) Influence of the degree of perlite expansion on immobilization of *Acinetobacter junii*. Biochem Eng J 51(3):117–123. https://doi.org/10.1016/j.bej.2010.06.004
20. Josefsen KD, Nordborg A, Sletta H (2017) Bioconversion of phytosterols into androstenedione by *Mycobacterium*. Methods Mol Biol 1645:177–197. https://doi:10.1007/978-1-4939-7183-1_13
21. Kang M, Kim HW, Yu AR, Yang JS, Lee SH, Lee JW, Yoon HS, Lee BS, Park HW, Lee SK, Lee S, Whang J, Kim JS (2022) Comparison of macrophage immune responses and metabolic reprogramming in smooth and rough variant infections of *Mycobacterium mucogenicum*. Int J Mol Sci 23(5):2488. https://doi:10.3390/ijms23052488
22. Laveaga GS (2005) Uncommon trajectories: steroid hormones, Mexican peasants, and the search for a wild yam. Stud Hist Philos Biol Biomed Sci 36(4):743–760
23. Liu H, Xu L, Yao K, Xiong L, Tao X, Liu M, Wang F, Wei D (2018) Engineered 3-ketosteroid 9α-hydroxylases in *Mycobacterium neoaurum*: an efficient platform for production of steroid drugs. Appl Environ Microbiol 84(14):e02777–e02717
24. Llanes N, Fernandes P, Léon R, Cabral JMS, Pinheiro HM (2001) Conversion of β-sitosterol by *Mycobacterium* sp. NRRL B-3805 cells immobilized on celite supports. J Mol Catal B: Enzym 11(4):523–530. https://doi.org/10.1016/S1381-1177(00)00010-2
25. Lyew D, Guiot SR, Monot F, Fayolle-Guichard F (2007) Comparison of different support materials for their capacity to immobilize *Mycobacterium austroafricanum* IFP 2012 and to adsorb MtBE. Enzyme Microb Technol 40(6):1524–1530. https://doi.org/10.1016/j.enzmictec.2006.10.040

26. Malaviya A, Gomes J (2008) Androstenedione production by biotransformation of phytosterols. Bioresour Technol 99(15):6725–6737
27. Mancilla RA, Little C, Amoroso A (2018) Efficient bioconversion of high concentration phytosterol microdispersion to 4-androstene-3,17-dione (AD) by *Mycobacterium* sp. B3805. Appl Biochem Biotechnol 185(2):494–506. https://doi:10.1007/s12010-017-2665-3
28. Molchanova M, Andryushina V, Savinova T, Stytsenko T, Rodina N, Voishvillo N (2007) Preparation of androsta-1,4-diene-3,17-dione from sterols using *Mycobacterium neoaurum* VKPM Ac-1656 strain. Russ J Bioorg Chem 33(3):354–358
29. Monu E, Blank G, Holley R, Zawistowski J (2008) Phytosterol effects on milk and yogurt microflora. J Food Sci 73(3):M121–M126. https://doi:10.1111/j.1750-3841.2008.00668.x
30. Pan X, Zhang Y, He C, Li G, Ma X, Zhang Q, Liu L, Lan M, Jiao Y (2022) Enhancement of anaerobic fermentation with corn straw by pig bone-derived biochar. Sci Total Environ 829:154326. https://doi:10.1016/j.scitotenv.2022.154326
31. Saab HB, Fouchard S, Boulanger A, Llopiz P, Neunlist S (2010) Performance of *Luffa cylindrica* as an immobilization matrix for the biotransformation of cholesterol by *Mycobacterium* species. Biocatal Biotransform 28(5–6):387–394. https://doi:10.3109/10242422.2010.537326
32. Shao M, Zhang X, Rao Z, Xu M, Yang T, Li H, Xu Z (2015) Enhanced production of androst-1,4-diene-3,17-dione by *Mycobacterium neoaurum* JC-12 using three-stage fermentation strategy. PLoS ONE 10(9):e0137658. https://doi:10.1371/journal.pone.0137658
33. Shen Y, Wang M, Li H, Wang Y, Luo J (2012) Influence of hydroxypropyl-β-cyclodextrin on phytosterol biotransformation by different strains of *Mycobacterium neoaurum*. J Ind Microbiol Biotechnol 39(9):1253–1259
34. Su L, Xu S, Shen Y, Xia M, Ren X, Wang L, Shang Z, Wang M (2020) The sterol carrier hydroxypropyl-β-cyclodextrin enhances metabolism of phytosterols by *Mycobacterium neoaurum*. Appl Environ Microbiol 86(15):e00441–e00420. https://doi:10.1128/aem.00441-20
35. Wang D, Zhang J, Cao DD, Wang X, Wei D (2021) Identification and in situ removal of an inhibitory intermediate to develop an efficient phytosterol bioconversion process using a cyclodextrin-resting cell system. RSC Adv 11(40):24787–24793. https://doi:10.1039/d1ra02774c
36. Wang J, Hu Y, Qiu C, Fan H, Yue Y, Jiao A, Xu X, Jin Z (2018) Immobilized cells of *Bacillus circulans* ATCC 21783 on palm curtain for fermentation in 5 L fermentation tanks. Molecules 23(11):2888. https://doi:10.3390/molecules23112888
37. Wendhausen R, Frigato M, Fernandes P, Carvalho C, Cruz A, Pinheiro H, Cabral J (2005) Chrysotile as a support for the immobilisation of *Mycobacterium* sp. NRRL B-3805 cells for the bioconversion of β-sitosterol in an organic-aqueous two-liquid phase system. J Mol Catal B: Enzym 32(3):61–65
38. Zhang X, Liu W, Cai J, Huang J, Qiu X-q (2019) Equip the hydrogel with armor: strong and super tough biomass reinforced hydrogels with excellent conductivity and anti-bacterial performance. J Mater Chem A 7(47):26917–26926. https://doi:10.1039/C9TA10509C

39. Zhang Y, Zhou X, Yao Y, Xu Q, Shi H, Wang K, Feng W, Shen Y (2021) Coexpression of VHb and MceG genes in *Mycobacterium* sp. Strain LZ2 enhances androstenone production via immobilized repeated batch fermentation. Bioresour Technol 342:125965. https://doi:10.1016/j.biortech.2021.125965
40. Zhao A, Zhang X, Li Y, Wang Z, Lv Y, Liu J, Alam MA, Xiong W, Xu J (2021) Mycolicibacterium cell factory for the production of steroid-based drug intermediates. Biotechnol Adv 53:107860. https://doi:10.1016/j.biotechadv.2021.107860
41. Zhao W, Xie H, Zhang X, Wang Z (2022) Crystal substrate inhibition during microbial transformation of phytosterols in Pickering emulsions. Appl Microbiol Biotechnol 106(7):2403–2414. https://doi:10.1007/s00253-022-11889-z
42. Zhou X, Zhang Y, Shen Y, Zhang X, Zan Z, Xia M, Luo J, Wang M (2020) Efficient repeated batch production of androstenedione using untreated cane molasses by *Mycobacterium neoaurum* driven by ATP futile cycle. Bioresour Technol 309:123307. https://doi:10.1016/j.biortech.2020.123307

Figures

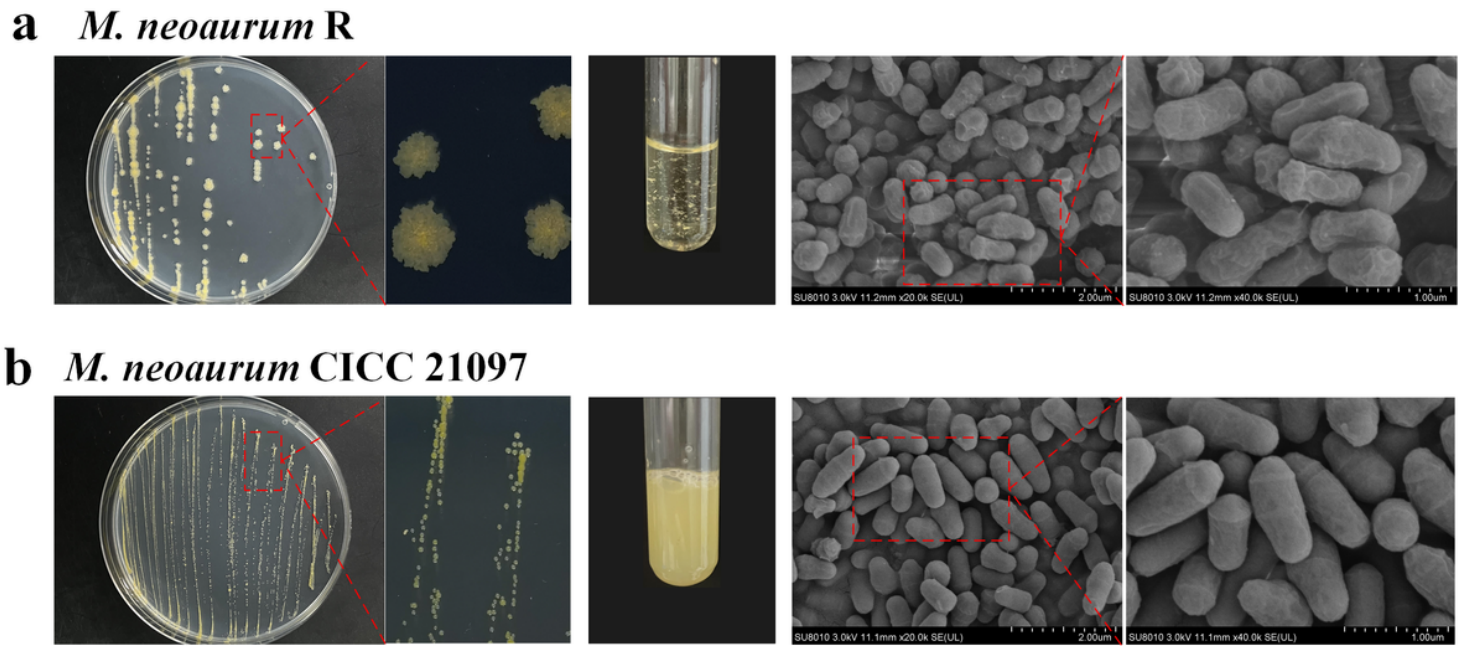

Figure 1

Characterization of rough morphotype *M. neoaurum* R and smooth morphotype *M. neoaurum* CICC 21097. **a** *M. neoaurum* R colonies on LB agar, *M. neoaurum* R cultured in LB medium with shaking, and SEM images of *M. neoaurum* R with magnifications of ×20 000 and ×40 000. **b** *M. neoaurum* CICC 21097 colonies on LB agar, *M. neoaurum* CICC 21097 cultured in LB medium with shaking, and SEM images of *M. neoaurum* CICC 21097 with magnifications of ×20 000 and ×40 000

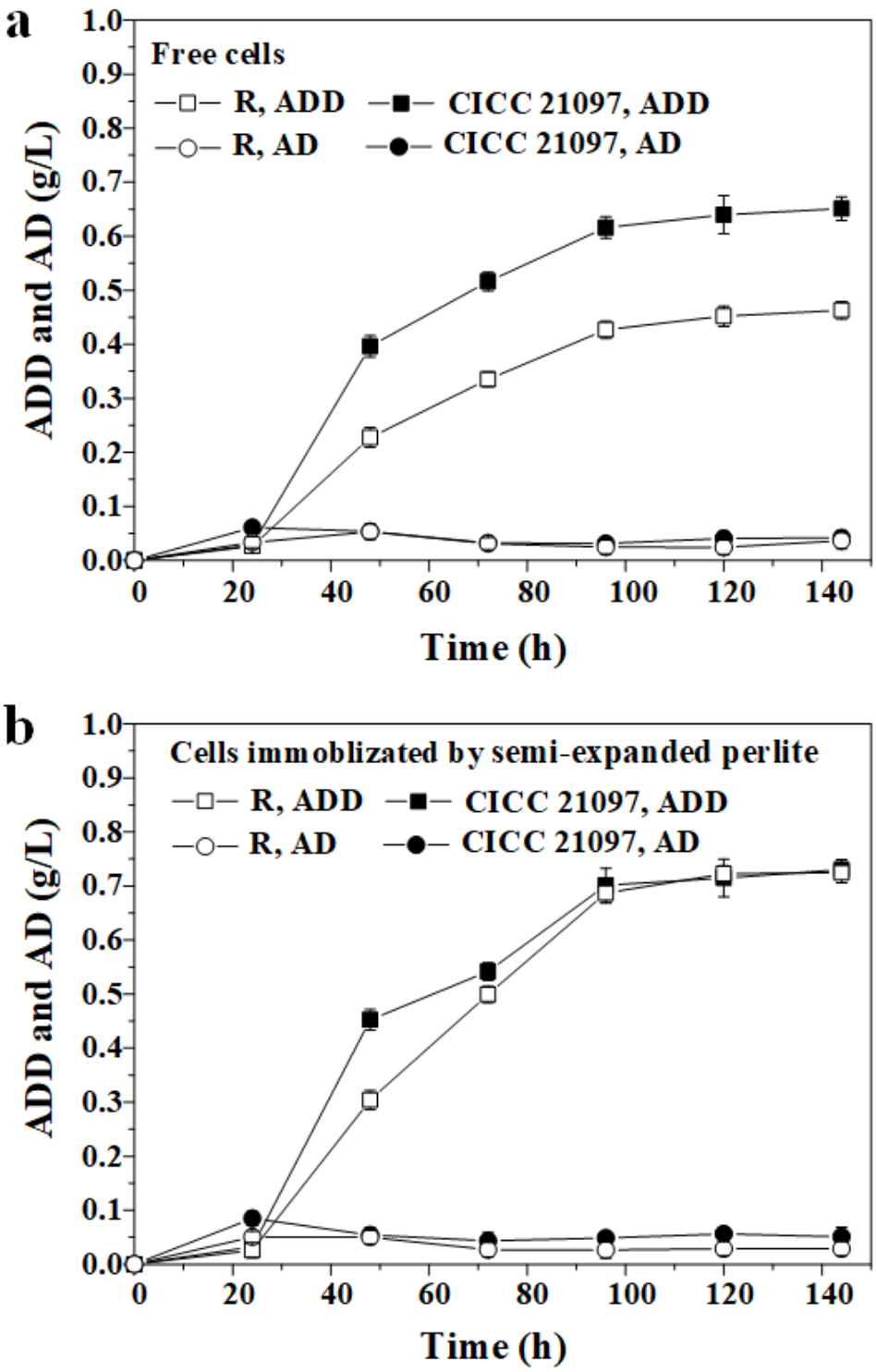

Figure 2

Comparison of androstadienedione (ADD) productions of *M. neoaurum* R and *M. neoaurum* CICC 21097. **a** The ADD and androstenedione (AD) productions by the free cells of *M. neoaurum* R and *M. neoaurum* CICC 21097 in fermentation medium. **b** The ADD and AD production by *M. neoaurum*R and *M. neoaurum* CICC 21097 in fermentation medium in the present of semi-expanded perlite.

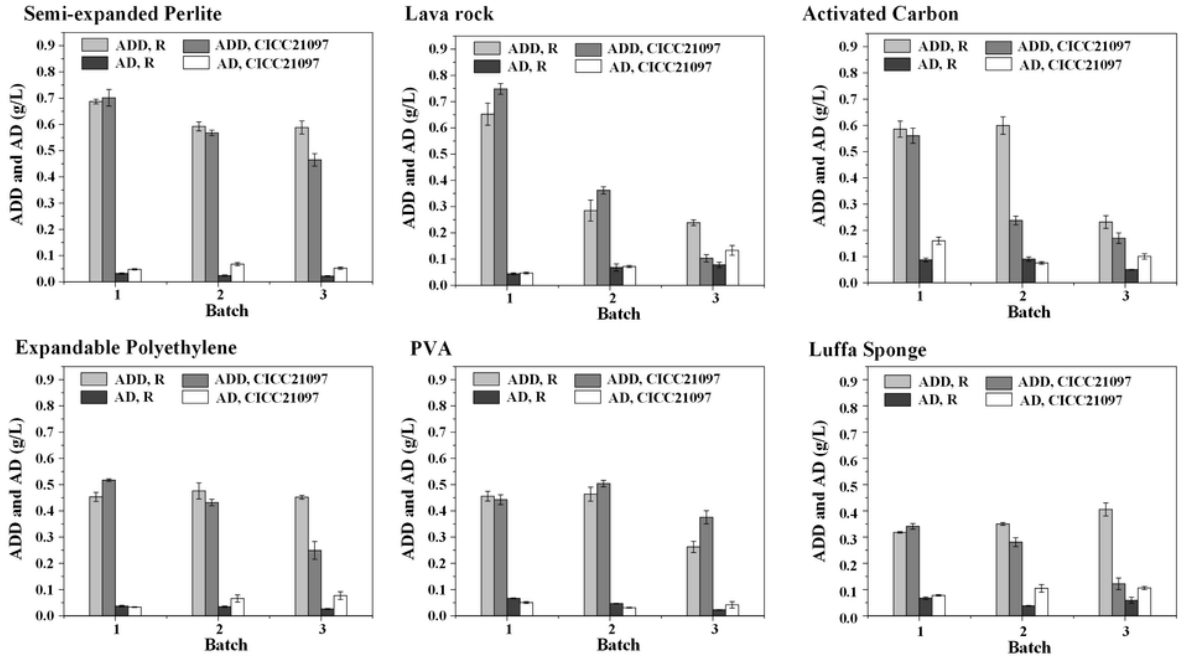

Figure 3

Repeated-batch fermentations of *M. neoaurum* R and *M. neoaurum* CICC 21097 immobilized by semi-expanded perlite, lava rock, activated carbon, expandable polyethylene, PVA hydrogel or luffa sponge.

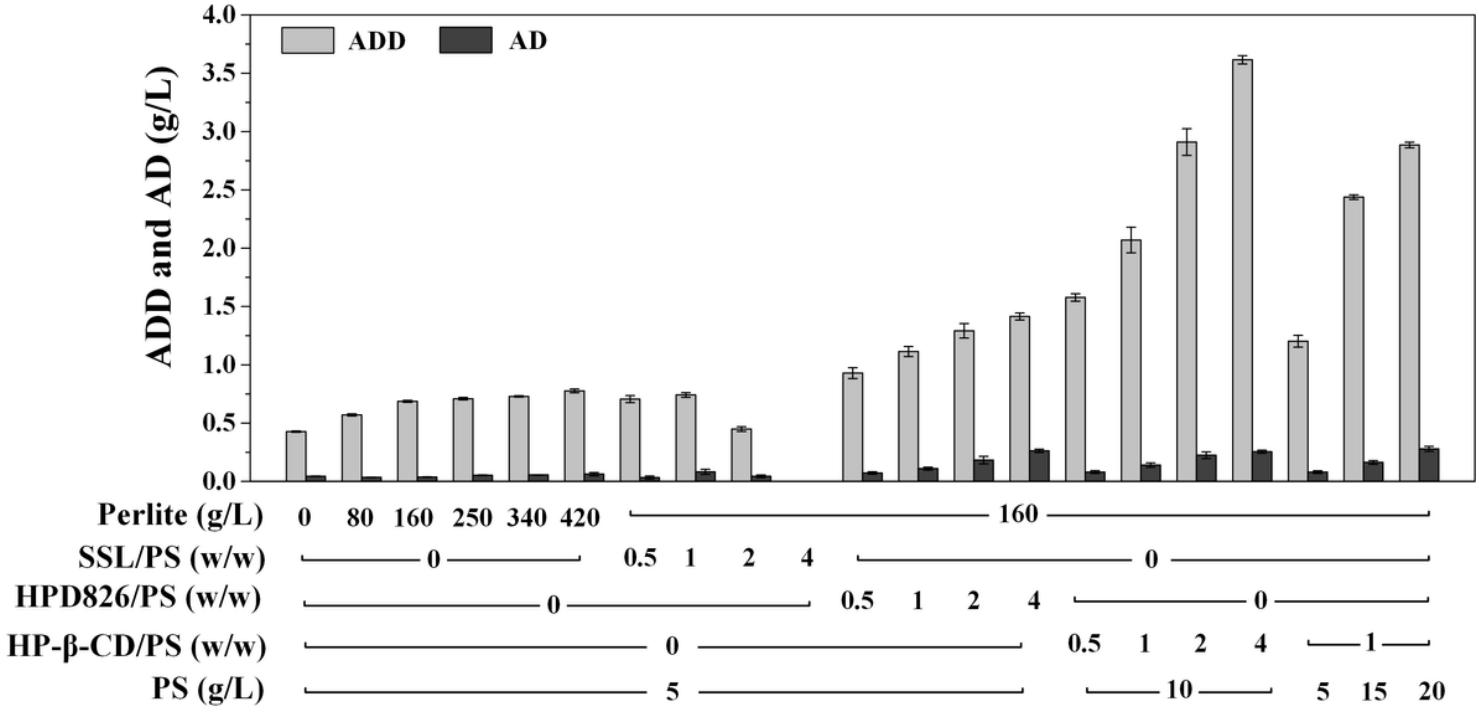

Figure 4

Determination of the optimal amounts of semi-expanded perlite, phytosterols and the co-solvents for phytosterols for the ADD production of immobilized *M. neoaurum* R using OFAT method. The investigated co-solvents were sodium stearoyl lactylate (SSL), macroporous resin HPD826 and HP-β-CD.

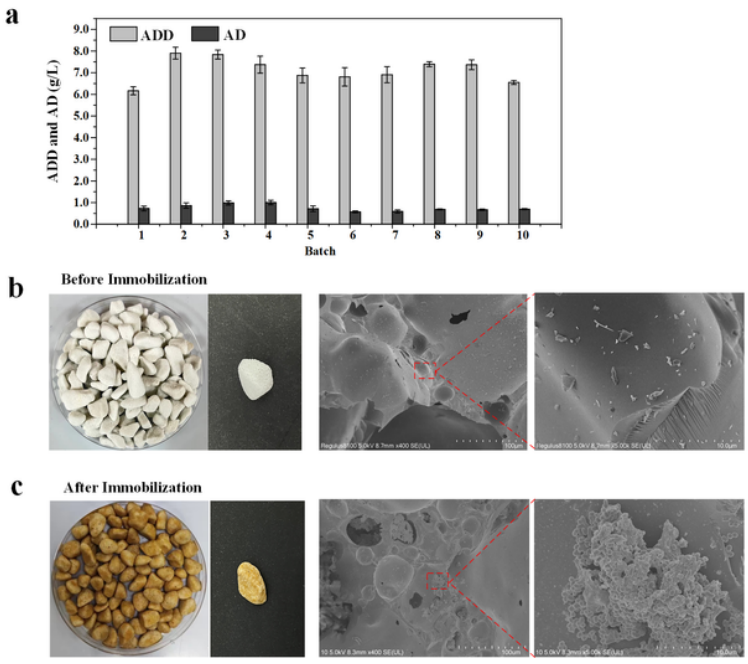

Figure 5

Extended repeated-batch fermentation of *M. neoaurum* R immobilized by semi-expanded perlite. **a** The ADD productions of ten-repeated-batch fermentation by immobilized *M. neoaurum* R in optimum medium. **b** Characterization of semi-expanded perlite. The magnifications of the SEM images were ×400 and ×5 000. **c** Characterization of semi-expanded perlite harboring immobilized *M. neoaurum* R. Sample were collected after ten-repeated-batch fermentation and the magnifications of the SEM images were ×400 and ×5 000.